2D melting and motility induced phase separation in Active Brownian Hard Disks and Dumbbells

Pasquale Digregorio, Demian Levis, Antonio Suma, Leticia Cugliandolo, Giuseppe Gonnella, Ignacio Pagonabarraga

2D melting and motility induced phase separation in Active Brownian Hard Disks and Dumbbells

IOP Conf. Series: Journal of Physics: Conf. Series 1163 (2019) 012073 doi:10.1088/1742-6596/1163/1/012073

2D melting and motility induced phase separation in Active Brownian Hard Disks and Dumbbells

Pasquale Digregorio[1], Demian Levis[2,3], Antonio Suma[4,5], Leticia F. Cugliandolo[6], Giuseppe Gonnella[1], Ignacio Pagonabarraga[2,3]

[1] Dipartimento di Fisica, Università degli Studi di Bari and INFN, Sezione di Bari, via Amendola 173, Bari, I-70126, Italy
[2] CECAM Centre Européeen de Calcul Atomique et Moléculaire, Ecole Polytechnique Fédérale de Lausanne, Batochimie, Avenue Forel 2, 1015 Lausanne, Switzerland
[2] UBICS University of Barcelona Institute of Complex Systems, Martí i Franquès 1, E08028 Barcelona, Spain
[4] SISSA - Scuola Internazionale Superiore di Studi Avanzati, Via Bonomea 265, 34136 Trieste, Italy
[5] Institute for Computational Molecular Science, Temple University, Philadelphia, PA 19122, USA
[6] Sorbonne Université, Laboratoire de Physique Théorique et Hautes Energies, CNRS UMR 7589, 4 Place Jussieu, 75252 Paris Cedex 05, France

Abstract. Recently, we characterized the complete phase transition diagram in the ϕ-Pe parameter space for two models of active brownian particles in two dimensions. These models are composed of hard disks and dumbbells, respectively, the former being isotropic and the latter anisotropic. Here, we want to outline all the most significant features of these two paradigmatic models and compare them.
Remarkably, the phase diagrams of the two models are affected differently by the introduction of activity. Disks present a two-stage melting scenario from Pe=0 to about Pe=3, with a first order phase transition between liquid and hexatic and a Berezinskii-Kosterlitz-Thouless transition between hexatic and solid. At higher activities, the three phases are still observed, but the transition between liquid and hexatic becomes a BKT transitions without a distinguishable coexistence region. Dumbbells, instead, present a macroscopic coexistence between hexatically ordered regions and disordered ones, over a finite interval of packing fractions, for all activities, included Pe=0, without any observable discontinuity in the behavior upon increasing Pe.

1. Introduction

Active materials evolve out of thermal equilibrium because their constituents are able to extract energy from the environment and inject it into the system, breaking detail balance [1]. Among others, Active Brownian Particles (ABP) model constitutes a standard paradigmatic model to study the impact of activity on soft matter [2, 3, 4]. For many of the active systems cited above, self-propulsion is able to trigger a motility-induced phase separation (MIPS) between a low-density gas-like phase and dense stable aggregates [5], reminiscent of the equilibrium liquid-gas transition but in the absence of cohesive forces and without a thermodynamic framework to support it [6, 7].

It is worth saying that the most intriguing phenomena induced by activity, as well as the most promising experimental applications, concern systems confined in 2D layers. Being interested

in further exploring aggregation phenomena and thermodynamic phases of passive and active two-dimensional systems at any finite density [8, 9, 10] and trying to establish a reference phase diagram for active matter, we naturally faced the long debated problem, still not fully understood, of the melting transition in two dimensions. .

While phase transitions in 2D systems with short-range interactions do not involve any spontaneous symmetry breaking mechanism [11], also ordered crystal-like phases have long been known to exist [12]. A general scenario was proposed to explain solidification in two dimensions by Halperin, Nelson and Young [13, 14, 15], according to which the ordering transition occurs in two steps: one from the isotropic liquid to a hexatic phase, with short-range translational order and quasi-long-range orientational order, and a second one from the hexatic to the solid, characterized by quasi-long-range translational order and a true long-range hexatic one. Both of this two transition are Berezinskii-Kosterlitz-Thouless (BKT) transitions, mediated by the unbinding of topological defects. Very recently, numerical simulations [16, 17, 18] and experimental results [19] reached a consistent understanding of the full melting transition for hard disks, which is still a two-step transition, but with a first-order liquid-hexatic transition and a BKT hexatic-solid one.

2. Methods

2.1. Active brownian disks

Active brownian disks constitute the simplest model of self-propelled brownian isotropic particles. The stochastic equations of motion for N repulsively interacting hard disks of mass m, self-propelled by an active force $\mathbf{F}_{\rm act}$ constant in modulus and directed along $\mathbf{n}_i =$

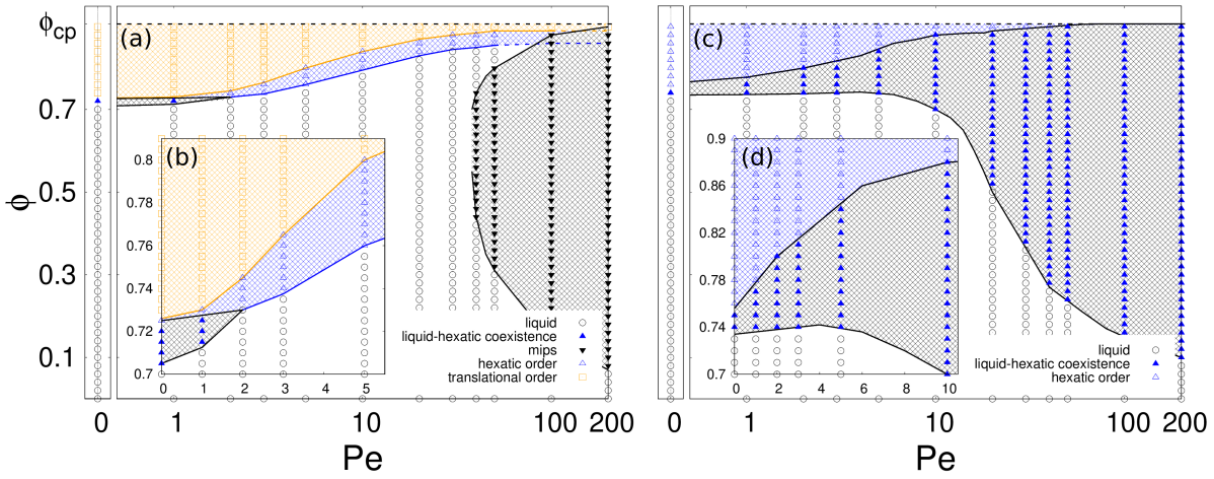

Figure 1. (a) Phase diagram of active brownian disks evolving according to eq. 1. Figure adapted from [20]. Symbols are used to point out the simulations performed. Black empty circles are shown in the liquid phase, blue empty triangles in the hexatic one, orange empty squares in the solid one. Filled symbols are used for the coexistence regions, circles for the low-Pe liquid-hexatic coexistence, triangles for the MIPS. (b) Enlargement of the small activity region across the coexistence. (c) Phase diagram of active brownian dumbbells (see eq. 2), adapted from [21]. Filled blue triangles are used here in the whole connected coexistence region. (d) Zoom of the coexistence region at low Pes.

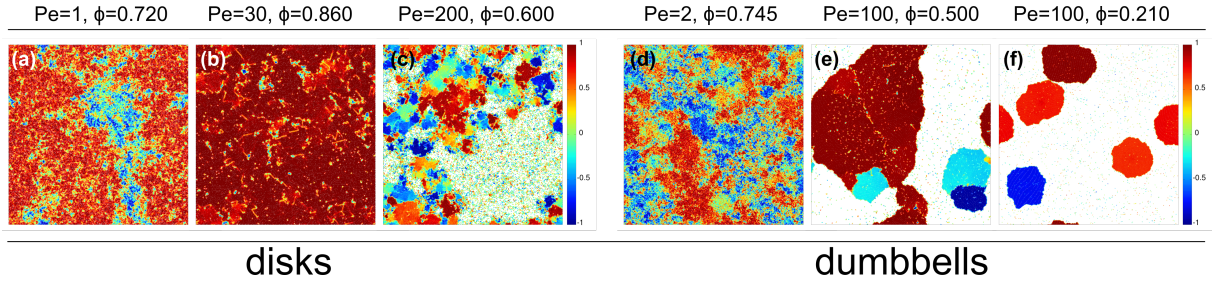

Figure 2. Color representation of the local hexatic parameter ψ_{6j} for disks (left) and dumbbells (right) and for cases given in the labels above the pictures. See the text for details about the color code. The following regions of the phase diagram are shown for disks: (a) liquid-hexatic coexistence at low Pe; (b) hexatic phase at intermediate Pe; (c) MIPS region at high Pe; and for dumbbells: (d) coexistence region at low Pe; (e) MIPS at high Pe, in the middle of the coexistence curve; (f) MIPS at high Pe, close to the lower limit of the coexistence region.

$(\cos\theta_i(t), \sin\theta_i(t))$, are:

$$m\ddot{\mathbf{r}}_i = -\gamma\dot{\mathbf{r}}_i + F_{\rm act}\mathbf{n}_i - \boldsymbol{\nabla}_i \sum_{j(\neq i)}^{N} U(r_{ij}) + \boldsymbol{\xi}_i \ , \qquad \dot{\theta}_i = \eta_i \ , \tag{1}$$

with $\mathbf{r}_i$ the position of the center of the i-th particle, $r_{ij} = |\mathbf{r}_i - \mathbf{r}_j|$ the inter-particle distance. The inter-particle potential is the short-range purely repulsive potential $U(r) = 4\varepsilon[(\sigma/r)^{64} - (\sigma/r)^{32}] + \varepsilon$ if $r < \sigma_d = 2^{1/32}\sigma$, and 0 otherwise, where σ_d is the diameter of the disks.
The terms $\boldsymbol{\xi}$ and η are zero-mean independent Gaussian noises that verify $\langle \boldsymbol{\xi}_i(t)\boldsymbol{\xi}_j(t')\rangle = 2\gamma k_B T\delta_{ij}\delta(t-t')\mathbf{1}$, $\langle \eta_i(t)\,\eta_j(t')\rangle = 2D_\theta\delta_{ij}\delta(t-t')$, with $D_\theta = 3k_BT/\gamma\sigma_d^2$. The units of length, mass and energy are given by σ_d, m and ε, and are typically set to one. Two relevant parameter of the model are the surface fraction occupied by the particles $\phi = \pi\sigma_d^2 N/(4V)$, where $V = L^2$ is the system's surface, and the Péclet number $\mathrm{Pe} = F_{\rm act}\sigma_d/(k_BT)$, which measures the ratio between the work done by the active force and the thermal energy K_BT. We tune L and $F_{\rm act}$ at fixed $\gamma = 10$ and $k_BT = 0.05$, according to the value of ϕ and Pe that we want to obtain, in order to explore the whole space parameter. This choice of the values for friction coefficient and temperature ensures the overdamped regime, as commonly used in the field and justified by the low-Re regime of most experiments.

The equation of motions are integrated numerically, using the software LAMMPS [22], with a velocity Verlet algorithm and an additional Langevin-type thermostat.

2.2. Active dumbbells

Dumbbells are diatomic molecules consisting of two identical disks of diameter σ_d. The equations of motion for $2N$ disks are:

$$m\ddot{\mathbf{r}}_i = -\gamma\dot{\mathbf{r}}_i + \mathbf{F}_{\rm act} - \boldsymbol{\nabla}_i \sum_{j(\neq i)}^{2N} U(r_{ij}) + \boldsymbol{\chi}_i \ . \tag{2}$$

The potential is the same as the one defined above, while $\boldsymbol{\chi}_i$ are uncorrelated Gaussian noises with zero mean and variance $2\gamma k_BT$. The active force has constant magnitude $F_{\rm act}$ and is kept along the tail-to-head direction. The bond between the disks of each dumbbell are kept rigid at

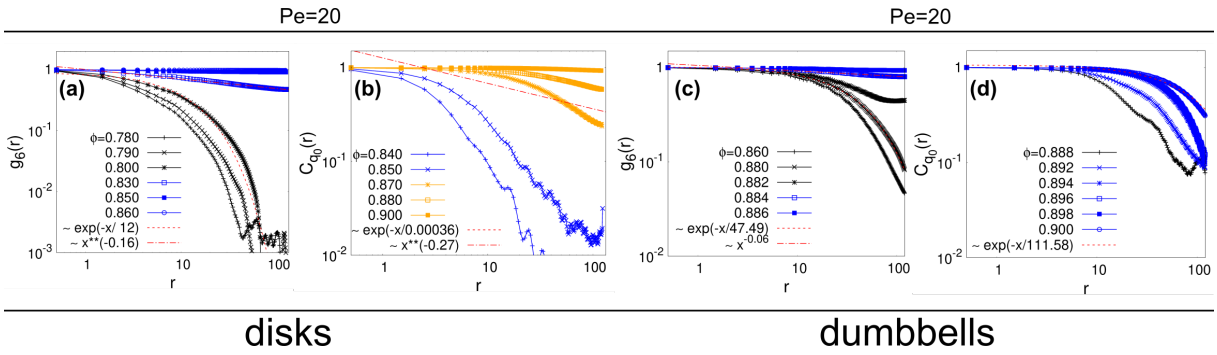

Figure 3. Correlation functions at fixed Pe= 20 and different ϕs as defined in the keys. (a) Hexatic correlations functions for disks across the liquid-hexatic transition; (b) translational correlation functions for disks across the hexatic-solid transition; (c) hexatic correlation functions for dumbbells across the liquid-hexatic transition; (d) translational correlation functions for dumbbells up to the close-packing limit.

a distance σ_d using a RATTLE scheme [23]. The surface fraction is $\phi = \pi\sigma_d^2(2N)/(4V)$, while the Péclet number is $\mathrm{Pe} = 2F_{\mathrm{act}}\sigma_d/(k_BT)$.
Note that the dumbbell model differ from colloids in the way the rotational diffusion is implemented. While the latter is unaffected by the surrounding particles, because the equation of motion for θ is independent from the atoms positions, dumbbells rotate due to the combination of the noise of the dimers. Thus, when dumbbells start to cluster together, they will not be able to rotate.
The equation of motions are integrated in the same way as the ones of colloids.

3. Phase diagram of the two models

The phase diagram for isotropic particles (Fig. 1(a,b)) has been established according to a systematic evaluation of several quantities. As described in details in [20], we used local surface fraction pdfs and virial pressure for self-propelled disks defined as in [6] to provide the limits of the coexistence regions throughout the parameters space. Spatial correlation functions $g_6(r)$ for the two-point correlation of the local hexatic parameter $\psi_6(\mathbf{r}_j) = N_j^{-1}\sum_{k=1}^{N_j} e^{\mathrm{i}6\theta_{jk}}$ and finite size analysis of its 4-th order cumulant allowed us to distinguish between liquid structure and hexatic one, and consequently to locate the liquid-hexatic transition for all values of Pe. Besides, correlation functions $C_{\mathbf{q_0}}(r)$ of local translational order parameter $e^{\mathrm{i}\mathbf{q_0}\cdot\mathbf{r_i}}$, being $\mathbf{q_0}$ the maximum of the diffraction peak in the reciprocal space, have been used to identify hexatic-solid transition.

Both the two peaks structure in density pdfs and the double loop shape in the equation of state consistently demonstrate that the liquid-hexatic transition in the passive limit is a first order phase transition, as expected from repulsive disk with a $\sim r^{-64}$ repulsive interaction [18], and that, notably, the first-order nature of this phase transition is preserved after bringing the system out of equilibrium by adding non-zero small activity, up to Pe$\sim$ 3. For larger Pes liquid-to-hexatic transition undergoes a crossover to a continuous transition. On the other hand, upon increasing activity from the passive limit, the BKT nature of hexatic-solid transition is maintained at all finite activities. Activity has the effect to destabilize the two ordered phases and, as a consequence, hexatic and solid are pushed towards higher surface fraction. Nevertheless, remarkably, both hexatic and solid phases are demonstrated to exist as stable thermodynamic phases up to very high activities. This can be directly observed from the hexatic and translational correlation functions shown, for fixed Pe= 20 in Fig. 3(a,b). Note that above $\phi \gtrsim 0.800$ the hexatic correlation length diverges as expected in the hexatic phase

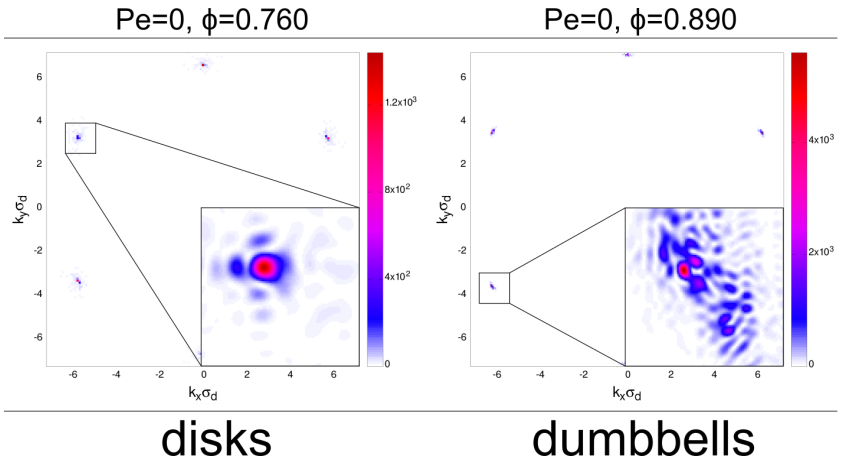

Figure 4. Static structure factor $S(q) = N^{-1} \sum_{i,j} e^{i\mathbf{q}\cdot(\mathbf{r}_i - \mathbf{r}_j)}$ for ordered configurations of disks and dumbbells, with an enlargement of one of the six peaks.

from Halperin-Nelson theory. Above $\phi \gtrsim 0.870$ also the positional correlation length diverges indicating the emergence of quasi-long-range translational order.

Hexatic order for self-propelled disks can also be inferred qualitatively by providing a color map for the local hexatic parameter defined before. We include some examples of this map in Fig. 2 for few representative cases at different points in the Pe-ϕ space reported within the figure. The color scale refers to the projection of the local hexatic parameter along the direction in the complex plane of the sample average of the parameter itself. The specific nature of the configurations shown in Fig. 2 is provided within the caption.

For what concerns dumbbells, we studied the phase diagram in great details in [21], focusing on the emerging relations between the two-dimensional phase transition scheme for passive dumbbells and the motility-induced phase separation. As clearly shown in Fig. 1(c,d), we found a strongly different, but still much interesting scenario, never seen with disks, demonstrating at least that MIPS is a strong system-dependent phenomenon.

We used the same quantities described above for the disks in order to explore extensively the parameter space. In the limit of passive dumbbells we observed that, similarly to isotropic particles, our molecules undergo a first order phase transition between isotropic liquid and a hexatic phase for the mutual orientation of the centers of mass of the single beads. This represents a notable extension to molecular systems of the most recent results obtained for hard disks [17, 19] and is a novelty in the understanding of the nature of 2d melting.

The most remarkable point we found is that, turning on activity and increasing Pe from the passive limit we did not find any finite critical value of activity which triggers the motility-induced phase separation, since we observe macroscopic phase separation for each probed Pe value. As shown in Fig. 3(c), increasing the surface fraction and crossing the upper limit of the coexistence region, quasi-long-range orientational order arises in the system, revealing that coexistence is between a liquid-gas phase and a hexatic phase everywhere in the spanned activity range. Moreover, the finite range of packing fractions where liquid and hexatic coexist is continuously connected throughout the phase diagram, suggesting a crucial interplay between the liquid-hexatic first order phase transition and the motility-induced phase separation.

From both the phase diagram of Fig. 1(a,b) and translational correlation functions for dumbbells shown in Fig. 3(d) is worth noting that we did not find any certain evidence of the existence of a solid phase for dumbbells. Neither for passive molecules, nor with activity, we observe quasi-long-range positional order for the centers of mass of the beads. As explained

in [24], the reason for that comes from the shape of the objects in the system. Indeed, since each head-to-tail distance is fixed to the same value σ_d for all values of the global packing fraction, the beads cannot arrange on a perfect triangular lattice, as they are free to do in the disk geometry, at any global $\phi < \phi_{cp}(\sim 0.900)$. More quantitatively, the lack of positional order for dumbbells can be deduced from the the structure of the diffractions peaks in the reciprocal space for the ordered phase. In Fig. 4 the structure factor for passive disks in the solid phase and the one for passive dumbbells at very high packing fraction, close to the maximum packing value, shown the six-fold structure expected for a hexagonal packing. In the same figure is also shown an enlargement of the structure of the peaks used, as described before, for calculating the translational correlation function. While for the disks this peaks has a regular symmetric structure, as the power-law singularity expected in a 2D solid [14], for the dumbbells it is much more broadened. Clearly, the structure of the six peaks representing the triangular order for the beads merges with the internal structure of the molecules, strongly indicating the absence of quasi-long-range positional order.

4. Conclusions

This wide analysis of two of the most simple and representative models of active systems has revealed many interesting features both of 2D melting scenario for passive anisotropic objects and activity-driven aggregation. Furthermore, it inspires fundamental questions about the nature of the ordered phases in presence of activity and about the strong observed dependence of motility-induced phase separation on the shape of the self-propelled constituents. First, we aim to explore further the profound differences between active disks and dumbbells and establish stronger relationship between them. Moreover, would be of great relevance to investigate the role of topological defects in the active melting transitions, comparing the results with the general framework for defects of the KTHNY theory.

References

[1] Marchetti M C, Joanny J F, Ramaswamy S, Liverpool T B, Prost J, Rao M and Simha R A 2013 *Rev. Mod. Phys.* **85** 1143
[2] ten Hagen B, van Teeffelen S and Löwen H 2011 *J. Phys. C: Cond. Matt.* **23** 194119
[3] Romanczuk P, Bär M, Ebeling W, Lindner B and Schimansky-Geier L 2012 *Eur. Phys. J. Spec. Topics* **202** 1–162
[4] Cates M and Tailleur J 2013 *EPL* **101** 20010
[5] Cates M E and Tailleur J 2015 *Annu. Rev. Cond. Matt. Phys.* **6** 219
[6] Levis D, Codina J and Pagonabarraga I 2017 *Soft Matter* **13** 8113–8119
[7] Solon A P, Stenhammar J, Cates M E, Kafri Y and Tailleur J 2018 *Phys. Rev. E* **97** 020602
[8] Bialké J, Speck T and Löwen H 2012 *Phys. Rev. Lett.* **108** 168301
[9] Briand G and Dauchot O 2016 *Phys. Rev. Lett.* **117** 098004
[10] Klamser J U, Kapfer S C and Krauth W 2018 *arXiv:1802.10021*
[11] Mermin N D and Wagner H 1966 *Phys. Rev. Lett.* **17** 1133
[12] Alder B J and Wainwright T E 1962 *Phys. Rev.* **127** 359
[13] Kosterlitz J M and Thouless D J 1973 *J. Phys. C: Solid State Physics* **6** 1181
[14] Halperin B I and Nelson D R 1978 *Phys. Rev. Lett.* **41** 121
[15] Young A 1979 *Phys. Rev. B* **19** 1855
[16] Bernard E P, Krauth W and Wilson D B 2009 *Phys. Rev. E* **80** 056704
[17] Bernard E P and Krauth W 2011 *Phys. Rev. Lett.* **107** 155704
[18] Kapfer S and Krauth W 2015 *Phys. Rev. Lett.* **114** 035702
[19] Thorneywork A L, Abbott J L, Aarts D G A L and Dullens R P A 2017 *Phys. Rev. Lett.* **118** 158001
[20] Digregorio P, Levis D, Suma A, Cugliandolo L F, Gonnella G and Pagonabarraga I 2018 *Phys. Rev. Lett.* **121**(9) 098003
[21] Cugliandolo L F, Digregorio P, Gonnella G and Suma A 2017 *Phys. Rev. Lett.* **119** 268002
[22] Plimpton S 1995 *J. Comp. Phys.* **117** 1–19
[23] Allen M P and Tildesley D J 1989 *Computer simulation of liquids* (Oxford University Press)
[24] Petrelli I, Digregorio P, Cugliandolo L F, Gonnella G and Suma A 2018 *arXiv:1805.06683*